Modeling of Electron-Beam Welding to Determine the Weld Joints Parameters of Dissimilar Materials

Gleb Lvovich Permyakov, Tatiana Vasiljevna Olshanskaya, Vladimir Yakovlevich Belenkiy, Dmitriy Nikolaevich Trushnikov, Lev Nikolaevich Krotov

Perm National Research Polytechnic University, Komsomolsky Av., 29, Perm, 614990, Russian Federation.
gleb.permyakov@yandex.ru

Abstract: We developed a mathematical model for the approximate selection of modes of electron-beam welding (EBW) of dissimilar materials on the basis of the energy transfer equation with mixed boundary conditions and the two sets of thermophysical characteristics, which depend on the coordinates. The solution of the boundary value problem is received by the method of Green's functions using the program MathCAD 15.

1. Introduction

Many researchers have considered the problems, features, and mathematical description of the process of welding with deep penetration. We begin by discussing the physical fundamentals and general principles of the process [1, 2, 3].

Based on these principles, we developed different mathematical models, from simple models [1, 2, 4] to complex and numerical models [5, 6, 7, 8, 9]. Using these models, we describe processes such as the energy absorption of different types of radiation; hydrodynamic effects; crystallization processes; the evaporation of keyholes from channel walls; and the thermal effects associated with the reaction of evaporation vapors with molten metal. In addition, these models enable us to analyze phase transitions, the formation of welding stresses, and segregation.

The situation is more complicated when welding dissimilar materials, because most pairs of welded dissimilar metals or alloys are characterized by substantial differences in melting point, density, and coefficient of thermal properties. Some features and a simulation of welding dissimilar materials are discussed in several investigations [1, 2, 10].

The vast majority of current researchers prefer numerical modeling techniques of welding processes, but as practice shows, for engineering calculations enough analytical methods. We can note the following advantages of analytical methods [11]: 1) Analytical solutions are more informative than numerical; 2) Volume of computing does not depend on the values of the spatial and temporal coordinates (i.e. there is no accumulation of systematic calculated errors); 3) Analytical methods allow you to define solutions at any point, not just in the grid nodes; 4) Analytical methods allow us to calculate the value at one point, without resorting to the evaluation the values of decisions in other points, as it happens for solving difference schemes; 5) The possibility of using previously obtained solutions of particular tasks; 6) Possibility of analyzing and simplify solutions; 7) Possible to trace the influence of physical parameters, initial and boundary conditions on the nature of the solution.

And the decision was made to develop an analytical model of Electron-Beam welding to determine the parameters weld joints of dissimilar materials.

2. Mathematical Models

Thermal processes in welding have been conveniently described by the equation in the moving coordinate system with a fixed source. In the coordinate system, moving relatively on the x-axis with speed V, the heat equation becomes an equation of energy transfer and is written as:

$$\frac{\partial T}{\partial t} = a \cdot \left(\frac{\partial^2 T}{\partial x^2} + \frac{\partial^2 T}{\partial y^2} + \frac{\partial^2 T}{\partial z^2} \right) + V \frac{\partial T}{\partial x} + \frac{q}{c\rho}$$

The differential equation of energy transfer is a mathematical model of a whole class of phenomena regarding heat conduction. It has infinitely many solutions. It is necessary to acquire additional information not contained in the original differential equation to obtain one particular solution, which characterizes the specific process [11, 12]. These additional conditions, together with the differential equation, define a specific task:

1) The settlement scheme − infinite plate of thickness δ:

$$-\infty < x < \infty; \qquad -\infty < y < \infty; \qquad 0 < z < \delta$$

2) Boundary conditions of mixed type:

The boundary conditions of the second kind on the surface z = 0 and z = δ:

$$\left.\frac{\partial T}{\partial z}\right|_{z=0} = \left.\frac{\partial T}{\partial z}\right|_{z=\delta} = 0$$

x and y boundary conditions of the first kind are equal to 0;

3) Two sets of thermophysical characteristics: c1, λ1, ρ1, a1 and c2, λ2, ρ2, a2;

4) Temperature at the initial time is equal to 0.

Welding is carried out on a joint of the two materials (along the axis x, y = 0, z = 0) with speed V, power of electron beam q = IU, diameter of beam d, and welding time t.

Solving the boundary value problem was received by the Green's functions. The integral solution of the equation of energy transfer has the following form:

$$T(x,y,z,\tau) = \iiiint\limits_{\tau\,z\,y\,x} G(x,x',y,y',z,z',\tau) \cdot F(x,y,z,\tau)\partial x'\partial y'\partial z'\partial\tau$$

where $G(x,x',y,y',z,z',\tau)$ – Green's function, $F(x,y,z,\tau)$ – source function. It is known that Green's function admits that there is an incomplete separation of variables, which can be represented as the following product:

$$G(x,x',y,y',z,z',\tau) = G_x(x,x',\tau)G_y(y,y',\tau)G_z(z,z',\tau)$$

where:

$$G_x(x,x',\tau) = \frac{1}{2\cdot\sqrt{\pi a\tau}}\cdot\exp\left(-\frac{(x-x'+V\cdot\tau)^2}{4a\tau}\right)$$

$$G_y(y,y',\tau) = \frac{1}{2\cdot\sqrt{\pi a\tau}}\cdot\exp\left(-\frac{(y-y')^2}{4a\tau}\right)$$

$$G_z(z,z',\tau) = \frac{1}{2\cdot\sqrt{\pi a\tau}}\cdot\sum_{n=-\infty}^{\infty}\left(\exp\left(-\frac{(z-z'+2n\delta)^2}{4a\tau}\right) + \exp\left(-\frac{(z+z'+2n\delta)^2}{4a\tau}\right)\right)$$

The one-dimensional Green's functions are selected on the basis of the boundary conditions.

To assess the character of the distribution of the temperature fields at electron-beam welding, we can use a mathematical model, in which the thermal effect of the electron beam is considered as an impact that is continuous of the combined source [1, 2, 11]. In this study, we used two types of combined sources:

1) EBW with transverse beam oscillations relative to butt joint with the amplitude A – the normally distributed continuous source, which is linear in depth (along the axis z, length h) and linear along the axis y (length 2A), introduced at the coordinate origin acting throughout the period of time t:

$$F1(x,y,z,\tau) = \frac{q\eta}{c\rho}\cdot\left(\frac{k1}{2A}\cdot\delta(x')E(y')\delta(z')E(\tau) + \frac{k2}{2Ah}\cdot\delta(x')E(y')E(z')E(\tau)\right)$$

$$E(y') = \begin{cases}1\,\text{if}-A\leq y'\leq A\\0\,\text{if}\,A<y'<-A\end{cases}; E(z') = \begin{cases}1\,\text{if}\,0\leq z'\leq h\\0\,\text{if}\,h<z'<0\end{cases}; E(\tau) = \begin{cases}1\,\text{if}\,t0\leq\tau\leq t\\0\,\text{if}\,\tau>t\end{cases}$$

2) EBW with X-shaped beam oscillations with amplitude b – the normally distributed continuous source, which is linear in depth (along the axis z, length h) and rectangular (2b on 2b) on the surface, introduced at the coordinate origin acting throughout the period of time t:

$$F2(x,y,z,\tau) = \frac{q\eta}{c\rho}\cdot\left(\frac{k1}{4b^2}\cdot E(x')E(y')\delta(z')E(\tau) + \frac{k2}{4b^2h}\cdot E(x')E(y')E(z')E(\tau)\right)$$

$$E(x') = \begin{cases}1\,\text{if}-b\leq x'\leq b\\0\,\text{if}\,b<x'<-b\end{cases}; E(y') = \begin{cases}1\,\text{if}-b\leq y'\leq b\\0\,\text{if}\,b<y'<-b\end{cases};$$

$$E(z') = \begin{cases}1\,\text{if}\,0\leq z'\leq h\\0\,\text{if}\,h<z'<0\end{cases}; E(\tau) = \begin{cases}1\,\text{if}\,t0\leq\tau\leq t\\0\,\text{if}\,\tau>t\end{cases}$$

The distribution of beam power between the surface and the linear sources is considered at the expense of the introduction of the coefficients of energy distribution k1 and k2. The average value of the coefficients is as follows: k1=0,2…0,3 and k2=0,7…0,8.

To simulate the impact of the normal-circular source is calculated time of action of the fictitious source:

$$t0 = \frac{1}{4aK}$$

The magnitude of penetration of the linear source can be estimated by the depth of foundering, which is associated with the parameters of EBW in the following criterial equation [2]:

$$H = \frac{a^{(1-0,5k)}}{(\lambda\cdot T_m)^k}(\eta\cdot q)^k V^{0,5k-1}d^{-0,5k}$$

where $k = 0,68\cdot(\lambda\cdot T_m)^{0,15}$, a – thermal diffusivity, λ – thermal conductivity, T_m – melting temperature, η – effective efficiency, q – power heat flux, V – welding speed, d – diameter of the beam.

Thus, we write the integral solving the transport equation of energy for the function of the first source that describes the mathematical model EBW with transverse fluctuations in the beam as follows:

$$T1(x,y,z,\tau) = \frac{k1 \cdot q\eta}{8A\pi\lambda} \int_{t0}^{t} \frac{1}{\tau} \cdot \exp\left(-\frac{(x+V\cdot\tau)^2}{4a\tau}\right) \cdot \left(\begin{array}{c} erf\left(\dfrac{y+A}{2\cdot\sqrt{a\tau}}\right) - \\ -erf\left(\dfrac{y-A}{2\cdot\sqrt{a\tau}}\right) \end{array}\right) \cdot \sum_{n=-\infty}^{\infty} \exp\left(-\frac{(z+2n\delta)^2}{4a\tau}\right)\partial\tau +$$

$$+ \frac{k2 \cdot q\eta}{16Ahc\rho\cdot\sqrt{\pi a}} \cdot \int_{t0}^{t} \frac{1}{\sqrt{\tau}} \cdot \exp\left(-\frac{(x+V\cdot\tau)^2}{4a\tau}\right) \cdot \left(\begin{array}{c} erf\left(\dfrac{y+A}{2\cdot\sqrt{a\tau}}\right) - \\ -erf\left(\dfrac{y-A}{2\cdot\sqrt{a\tau}}\right) \end{array}\right) \cdot \sum_{n=-\infty}^{\infty} \left(\begin{array}{c} erf\left(\dfrac{z+h+2n\delta}{2\cdot\sqrt{a\tau}}\right) - \\ -erf\left(\dfrac{z-h+2n\delta}{2\cdot\sqrt{a\tau}}\right) \end{array}\right)\partial\tau$$

Similarly, we write the integral solution of the transport equation of energy for the function of the second source, which describes the mathematical model of EBW with X-shaped beam fluctuations, as follows:

$$T2(x,y,z,\tau) = \frac{k1 \cdot q\eta}{16b^2c\rho\cdot\sqrt{\pi a}} \cdot \int_{t0}^{t} \frac{1}{\sqrt{\tau}} \cdot \left(\begin{array}{c} erf\left(\dfrac{x+b+V\cdot\tau}{2\cdot\sqrt{a\tau}}\right) - \\ -erf\left(\dfrac{x-b+V\cdot\tau}{2\cdot\sqrt{a\tau}}\right) \end{array}\right) \cdot \left(\begin{array}{c} erf\left(\dfrac{y+b}{2\cdot\sqrt{a\tau}}\right) - \\ -erf\left(\dfrac{y-b}{2\cdot\sqrt{a\tau}}\right) \end{array}\right) \cdot \sum_{n=-\infty}^{\infty} \left(\exp\left(-\frac{(z+2n\delta)^2}{4a\tau}\right)\right)\partial\tau +$$

$$+ \frac{k2 \cdot q\eta}{32b^2hc\rho} \cdot \int_{t0}^{t} \left(\begin{array}{c} erf\left(\dfrac{x+b+V\cdot\tau}{2\cdot\sqrt{a\tau}}\right) - \\ -erf\left(\dfrac{x-b+V\cdot\tau}{2\cdot\sqrt{a\tau}}\right) \end{array}\right) \cdot \left(\begin{array}{c} erf\left(\dfrac{y+b}{2\cdot\sqrt{a\tau}}\right) - \\ -erf\left(\dfrac{y-b}{2\cdot\sqrt{a\tau}}\right) \end{array}\right) \sum_{n=-\infty}^{\infty} \left(\begin{array}{c} erf\left(\dfrac{z+h+2n\delta}{2\cdot\sqrt{a\tau}}\right) - \\ -erf\left(\dfrac{z-h+2n\delta}{2\cdot\sqrt{a\tau}}\right) \end{array}\right)\partial\tau$$

3. Materials and Technique

For the modeling of welding dissimilar materials, we must set the dependence of the thermophysical properties of the coordinates. Because the welding starts at coordinates y=0, on the surface of the estimated body (z=0), along the axis x, the interface between the two materials is the axis y. Accordingly, in the area lying to the left, if y<0 is assigned the values of thermophysical properties of the first material ($c1$, $\lambda1$, $\rho1$, $a1$), the area lying to the right, i.e., for y>0, is assigned the values of the thermophysical properties of the second material ($c2$, $\lambda2$, $\rho2$, $a2$). Assumptions assign the average value of thermophysical characteristics of materials at y=0. Chemical composition and thermophysical characteristics of welded materials are presented in Tables 1 and 2, respectively.

Table 1. Chemical composition of welded materials, %.

Steel		Bronze	
Fe	Base	Fe	0.08 max
C	0.09-0.14	Cr	0.4-1
Si	0.8 max	Cu	98.5-99.6
Mn	0.8 max	Zn	0.3 max
Ni	4.8-5.8	Impurities	0.5 max
S	0.025 max		
P	0.035 max		
Cr	20-22		
Ti	0.25-0.5		
Al	0.8 max		

Table 2. Thermophysical characteristics of welded materials.

Parameters	Steel	Bronze
Thermal conductivity coefficient λ, J / (s · m · K)	25	260
Density ρ, kg/m³	7650	8900
Heat capacity c, J / (kg · K)	528	480
Melting temperature, °C	~1500	~1080

The calculation of temperature fields was carried in the program MathCAD 15. The program consists of several stages, which are described as follows:

2) The assignment of variables of welding mode (accelerating voltage, beam current, beam diameter at the surface, welding speed, welding time) and thermal characteristics of welded materials (thermal conductivity, density, heat capacity).

2) The preliminary calculation of penetration depth on the basis of the initial data to determine the penetration linear source as well as the calculation of additional parameters (coefficient K concentration and the duration of the fictitious source t0).

3) The calculation of the temperature fields on the coordinate planes X-Y and Y-Z.

4. Results and Discussion

The calculated data was compared with the samples of welded steel (thickness – 7.5 mm) with bronze (thickness – 5.5 mm). The samples were welded by the following modes:

Sample 1: I=32…34mA; U=60kV; V=5mm/s; transverse oscillations.

Sample 2: I=32…35mA; U=60kV; V=5mm/s; X-shaped oscillations.

Sample 1. The calculated temperature fields in the X-Y plane at z = 0 are shown in Figure 1.
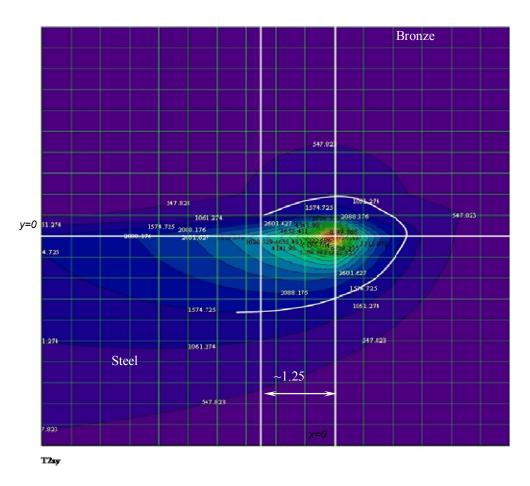

Fig. 1. Distribution of temperatures in the X-Y plane at z = 0 (1 division – 0.5 mm) for the first mode.

The maximum width of the zone heated to the melting point in the steel is offset relative to the coordinate x = 0. This is due to the large thermal inertia of the steel as compared with bronze. In order to obtain reliable data on the parameters of the joint, it is necessary to calculate the thermal fields in the Y-Z plane at x = 0 (for determining the width of the seam on bronze) and at displacement on 1.25 mm (for determining the width of the weld on steel). The calculated temperature fields in the Y-Z plane are presented in Figure 2.
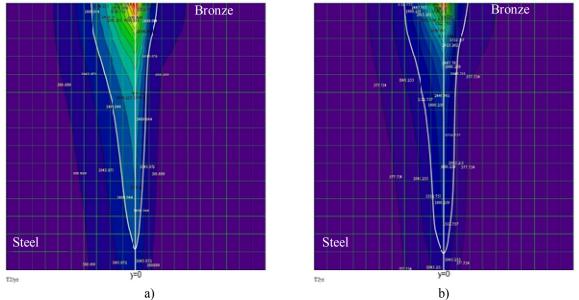
a)   b)

Fig. 2. Distribution of temperatures in the plane Y-Z for first mode:
a) at displacement along the x-axis; b) at x = 0.

By combining the charts of the temperature fields, we can acquire the real form of the seam. The result is presented in Figure 3.
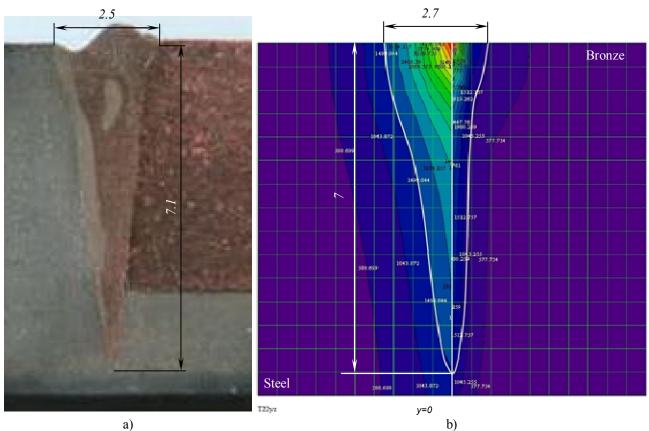

a)   b)
Fig. 3. Matching experimental (a) and calculated (b) weld joints for the first mode.

The discrepancy between the experimental and calculated data by the joint width is 8%, by the depth of penetration – 1.5%.

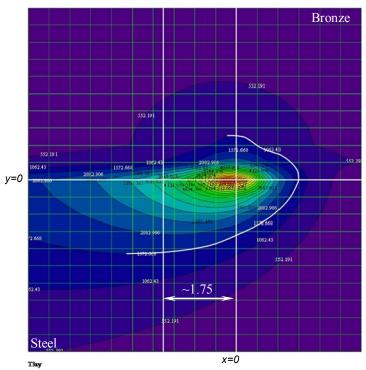**Sample 2.** The calculated temperature fields in the X-Y plane at z = 0 are presented in Figure 4.

Fig. 4. Distribution of temperatures in the X-Y plane at z = 0 (1 division – 0.5 mm) for the second mode.

To obtain data on the weld joint's parameters, it is necessary to calculate the thermal fields in the Y-Z plane at x = 0 (for determining the width of the seam on bronze) and at a displacement of 1.75 mm (for determining the width of the weld on steel). The calculated temperature fields in the Y-Z plane are presented in Figure 5.
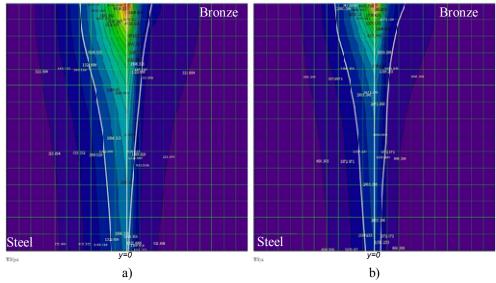

Fig. 5. Distribution of temperatures in the plane Y-Z for second mode:
a) at displacement along the x axis; b) at x = 0.

The combined charts and the results are presented in Figure 6.

Fig. 6. Matching experimental (a) and calculated (b) weld joints for the second mode.

Discrepancy between the experimental and calculated data by the joint width is 10%.

5. Conclusions:

1) We have developed a mathematical model for the calculation of temperature fields at electron-beam welding of dissimilar materials with an oscillating beam (with transverse and X-shaped oscillations).

2) The calculated temperature field obtained using this model provides insights into the geometry of the weld with an accuracy sufficient for engineering calculations.

3) This model can be used for the preliminary selection of the welding mode of dissimilar materials.

Corresponding Author:
Gleb L. Permyakov
The department for Welding Production and Technology of Constructional Materials
Perm National Research Polytechnic University
Perm, Perm, 614990, Russian Federation.
E-mail: gleb.permyakov@yandex.ru

References
1. Rykalin N. N., Uglov A. A., Zuev I. V. Fundamentals of electron-beam processing of materials. Moscow: Mashinostroyeniye, 1978. (in Russian)
2. Rykalin N. N., Uglov A. A., Zuev I. V., Kokora A. N. Laser and electron-beam processing of materials: Directory. Moscow: Mashinostroyeniye, 1985. (in Russian)
3. I. Y. Smurov, A.A. Uglov, A.M. Lashyn, P. Matteazzi, L. Covelli and V. Tagliaferri // Modelling of pulse-periodic energy flow action on metallic materials, International Journal of Heat and Mass Transfer. v.34, 1991, 961 –971.

4.   D. T. Swift-hook and a. E. F. Gick. Penetration Welding with Lasers // Welding Journal, 1973;52, p. 492 –499.
5.   A. Kaplan. A model of deep penetration laser welding based on calculation of the keyhole profile // J. Phys. D: Appt. Phys. 27 (1994) 1805-1814.
6.   T. DebRoy. Physical processes in fusion welding // Rev. Mod. Phys., Vol. 67, No. 1, January 1995, p.85 -112.
7.   W Sudniky, D Radajz and W Erofeew. Computerized simulation of laser beam welding, modeling and verification// J. Phys. D: Appl. Phys. 29 (1996) 2811–2817.
8.   Sudnik W., Erofeew W., Radaj D., Breitschwerdt S.Numerical simulation of weld pool geometry in laser beam welding // Journal

of Physics D: Applied Physics. 2000. T. 33. № 6. C. 662-671.
8.   Rai R., Palmer T.A., Elmer J.W., Debroy T. Heat transfer and fluid flow during electron beam welding of 304L stainless steel alloy// Welding Journal, March 2009, P. 54-s – 61-s.
9.   R. Rai, P. Burgardt, J. O. Milewski, T. J. Lienert and T. DebRoy Heat transfer and fluid flow during electron beam welding of 21Cr–6Ni–9Mn steel and Ti–6Al–4V alloy // J. Phys. D: Appl. Phys. 42 (2009) 025503.
10. Yazovskih V. M., Ttrushnikov D. N, Belenkiy V. Ya. Thermal processes in electron beam welding arc joints// Welding and diagnosis, No 5, 2012, P. 26-31 (in Russian).
11. Rykalin N. N. Calculations of thermal processes in welding. Moscow: Mashgiz. 1951. (in Russian).

3/1/2014